

Geophysical Research Letters®



RESEARCH LETTER

10.1029/2025GL117588

Key Points:

- Trends in precipitation volume, number of wet days, mean wet-day intensity in CONUS-404 are mostly statistically non-significant
- At the hourly resolution, significant increasing trends are found in the mean wet-hour intensity, mostly in the Midwest
- Spectral analysis shows that the magnitude of small-scale short-lived features has increased at a higher rate than that of larger features

Supporting Information:

Supporting Information may be found in the online version of this article.

Correspondence to:

C. Guilloteau,
cguillot@uci.edu

Citation:

Guilloteau, C., Chen, X., Leung, L. R., & Foufoula-Georgiou, E. (2025). Hourly precipitation intensities at 4-km resolution show statistically significant increasing trends from 1991 to 2022 in the CONUS-404 hydroclimate reanalysis. *Geophysical Research Letters*, 52, e2025GL117588. <https://doi.org/10.1029/2025GL117588>

Received 16 JUN 2025

Accepted 9 OCT 2025

Author Contributions:

Conceptualization: Clément Guilloteau, Efi Foufoula-Georgiou
Data curation: Clément Guilloteau, Xiaodong Chen
Formal analysis: Clément Guilloteau
Funding acquisition: Clément Guilloteau, L. Ruby Leung, Efi Foufoula-Georgiou
Methodology: Clément Guilloteau
Project administration: L. Ruby Leung, Efi Foufoula-Georgiou
Resources: Xiaodong Chen
Supervision: L. Ruby Leung, Efi Foufoula-Georgiou

© 2025 The Author(s).

This is an open access article under the terms of the [Creative Commons Attribution-NonCommercial License](https://creativecommons.org/licenses/by/4.0/), which permits use, distribution and reproduction in any medium, provided the original work is properly cited and is not used for commercial purposes.

Hourly Precipitation Intensities at 4-km Resolution Show Statistically Significant Increasing Trends From 1991 to 2022 in the CONUS-404 Hydroclimate Reanalysis

Clément Guilloteau¹ , Xiaodong Chen^{2,3} , L. Ruby Leung⁴ , and Efi Foufoula-Georgiou^{1,5} 

¹Department of Civil and Environmental Engineering, University of California Irvine, Irvine, CA, USA, ²School of Meteorology, University of Oklahoma, Norman, OK, USA, ³School of Civil Engineering and Environmental Science, University of Oklahoma, Norman, OK, USA, ⁴Atmospheric, Climate and Earth Sciences Division, Pacific Northwest National Laboratory, Richland, WA, USA, ⁵Department of Earth System Science, University of California Irvine, Irvine, CA, USA

Abstract Trends in hourly and daily precipitation statistics are studied using the CONUS-404 hydroclimate reanalysis at 4-km spatial resolution over the 1991–2022 period. Only a small fraction of CONUS shows statistically significant trends in the annual precipitation volume, number of wet days and mean wet-day intensity. Significant increasing trends are however found in the mean wet-hour precipitation intensity, with the trends being particularly pronounced in the Midwest. Fourier spectral analysis also attests for changes in the multiscale spatial and temporal organization of precipitation, and reveals that small-scale short-lived precipitation features have intensified at a higher rate than large-scale long-lived features. These results show that, even when no robust trend can be established from low-resolution data, clear trends may emerge at a higher resolution, demonstrating the need for high-resolution precipitation records for climate trend analysis.

Plain Language Summary This study analyzes trends in high-resolution (4-km and 1-hr) precipitation records from 1991 to 2022 over the Contiguous United States (CONUS). Over most of CONUS, the natural year-to-year variability dominates, and no robust trends emerge in the annual precipitation amount, number of wet days or mean intensity of wet days. When focusing however on the mean intensity of precipitation during wet hours, a clear intensification trend emerges over a large fraction of CONUS, and in the Midwest in particular. Further analyses reveal that the average amplitude of short-lived small-sized precipitation features has increased at a higher rate than that of large long-lived features.

1. Introduction

Increased atmospheric temperatures under global warming are expected to lead to increased atmospheric water content on average, as the Clausius-Clapeyron relationship establishes that the water-holding capacity of the atmosphere increases by 7% for every 1-K increase in temperature (North & Erukhimova, 2009). Increased atmospheric water content is ultimately expected to translate into increased precipitation volume on average. The response of precipitation characteristics to temperature changes is however strongly nonlinear. Precipitation also responds to changes in synoptic circulation controlling moisture transport, and changes in the thermodynamics of precipitating clouds involving moist convection processes. For these reasons, historical precipitation trends show contrasting patterns across different regions of the globe (Zaitchik et al., 2023). Moreover, global climate models often fail to accurately reproduce historical precipitation trends (Gu & Adler, 2023), and are often inconsistent with each other regarding future projected precipitation trends (John et al., 2022; Li et al., 2021). A consensus however seems to have emerged regarding high precipitation extremes, whose frequency and magnitude appear to increase consistently with temperature in both observations and models, across different regions of the globe, different observational data sets, and different climate models (e.g., O’Gorman, 2015; Papalexiou & Montanari, 2019; Thackeray et al., 2022). This increase in extremes is generally attributed to a shift toward a higher convective fraction and higher convective intensity in precipitating clouds in warmer climates. It has been sometimes labeled as “super-Clausius-Clapeyron” scaling, as its magnitude can exceed the 7%-per-K rate of the Clausius-Clapeyron relationship (Berg et al., 2013; Da Silva & Haerter, 2025; Fowler et al., 2021; Haerter & Berg, 2009; Panthou et al., 2014). Yet, when it comes to the identification of precipitation trends in historical data sets, several challenges arise. First, long-term continuous and homogeneous observational data sets are rare, because they require observation networks to be operated and maintained over several decades, and also because

Visualization: Clément Guilloteau,
Efi Foufoula-Georgiou
Writing – original draft:
Clément Guilloteau
Writing – review & editing:
Xiaodong Chen, L. Ruby Leung,
Efi Foufoula-Georgiou

technologies and measurement practices have been evolving over the years. Second, in many regions, precipitation statistics exhibit a high level of year-to-year variability, making it hard to separate trends from internal variability and produce statistically significant results, particularly when it comes to rare extreme events. For these reasons, historical precipitation trends reported in the literature are sometimes inconsistent across different data sets (e.g., Wang et al., 2023; Polasky et al., 2025), or between different studies (e.g., Emmanouil et al., 2022; Williams et al., 2024). Some studies have reported borderline levels of statistical significance (e.g., Nguyen et al., 2018; Nerantzaki et al., 2025). Finally, trends derived from inhomogeneous measurements over time (e.g., Zhang & Wang, 2023; Mascaro et al., 2025) are always equivocal.

The contiguous United States (CONUS) has been the focus of several studies seeking to identify trends in historical precipitation data sets (e.g., Feng et al., 2016; Hu et al., 2020). The recently released CONUS-404 hydroclimate reanalysis (Rasmussen, Chen, et al., 2023; Rasmussen, Liu, et al., 2023) offers new opportunities for analyzing the temporal and spatial variability of precipitation over an extensive 8M km² area for more than three decades, at an unprecedented 4-km and 1-hr resolution. In the present study we analyze precipitation trends in CONUS-404 from 1991 to 2022, focusing on the number of wet days and number of wet hours per year, the statistical distributions of daily and hourly intensities, and the fraction of wet hours above increasing intensity thresholds. Changes in the spatial and temporal organization of precipitation features across scales are further assessed through the Fourier power spectral density (PSD) of the precipitation fields. This study revisits the intensification of precipitation and the super-Clausius-Clapeyron scaling paradigms from a scale-intensity-dependent perspective rather than a solely intensity-dependent perspective. We choose to focus not only on the frequency and magnitude of precipitation extremes as most of the existing literature, but on assessing changes across the whole statistical distribution of hourly and daily precipitation intensities at 4-km resolution (and also at a degraded 40-km resolution) for more robust trend characterization and reduced sensitivity to internal variability.

2. Data and Methods

2.1. The CONUS-404 Downscaled Hydroclimate Reanalysis

The CONUS-404 high-resolution (4-km, 1-hr) hydroclimate reanalysis covering the 1980–2022 period has been released in December 2023 (Rasmussen, Chen, et al., 2023; Rasmussen, Liu, et al., 2023). This data set results from the dynamical downscaling of the ECMWF ERA-5 global reanalysis (Hersbach et al., 2020) through the WRF model. At 4-km resolution WRF explicitly resolves mesoscale processes and orographic forcing. Compared to gridded precipitation estimation products derived from observations only (ground stations, precipitation radars, and satellite measurements), CONUS-404 has advantages in terms of resolution (Guilloteau et al., 2017; Guilloteau & Foufoula-Georgiou, 2020) and continuity and homogeneity over space and time (Carvalho, 2020; Eldardiry et al., 2017; Rasmussen, Chen, et al., 2023). When it comes to trend analysis at multi-decadal scales, the stability over time of the observation system (gauge network, radar network or constellations of orbiting sensors) is critical. Technological evolutions of the sensors and the data processing chain, as well as variations over time in the number, location or orbit of the sensors are prone to introducing time-dependent artifacts in the records (Ayat et al., 2021; Doviak et al., 2000; Kidd et al., 2017; Petković et al., 2023; Rajagopal et al., 2021; Yang et al., 1998). While changes over time in the observation system may have only small effects when it comes to seasonal averages, the effects on high-order statistics (extreme statistics in particular) at the hourly time scale can be substantial (Guilloteau & Foufoula-Georgiou, 2023; Masunaga et al., 2019). Even if CONUS-404 is constrained by the observations assimilated in ERA-5, the distribution of precipitation within the simulation domain and the sub-daily variability are essentially the result of the thermodynamics of the WRF model, whose parametrization is homogeneous over the simulated period. CONUS-404 therefore inherits the advantages of numerical models in terms of homogeneity and consistency over time and space, while still relying on observations for its boundary conditions, allowing for realistic synoptic forcing and sub-seasonal to decadal variability and mitigating model biases (Rasmussen, Chen, et al., 2023).

Monthly precipitation statistics in CONUS-404 have been verified against the gauge-derived PRISM data set in Rasmussen, Chen, et al. (2023), and “close to zero” differences between CONUS-404 and PRISM are reported over most of CONUS. The largest monthly biases are overestimation in the coastal regions of the Pacific Northwest during winter months and underestimation over the Southeast during winter months. The local relative monthly biases always remain within an “acceptable” $\pm 30\%$ range. Focusing on mountain hydroclimate, Adhikari et al. (2024) found that CONUS-404 has the lowest biases on average among 16 dynamically downscaled climate

data sets evaluated against PRISM, and reported a 10%–20% overestimation of winter precipitation over mountains for CONUS-404. Further evaluation of CONUS-404 against gauge-radar data is provided in Supporting Information S1 to the present article, focusing specifically on its ability to capture month to month variations in the number of wet hours (Figures S5 and S6 in Supporting Information S1). The low biases of CONUS-404 in terms of monthly precipitation volume and its ability to accurately capture local month to month variations in the number of wet hours, combined with its temporal continuity and homogeneity, make it an ideal data set for the present analysis.

While the CONUS-404 data set extends back to 1980, the present study only utilizes data from 1991 to 2022. Limiting the analysis to the post-90's era allows to limit the potential influence of data artifacts in ERA-5 in the early years of the satellite era (Bromwich et al., 2024; Buschow, 2024), as well as data artifacts in the first six years of the CONUS-404 record (1980–1985), due to spinup issues with the WRF downscaling model (Rasmussen, Chen, et al., 2023).

2.2. Linear Trend Extraction Through Least Squares Regression

Precipitation statistics over the 1991–2022 period in CONUS-404 are first analyzed in terms of annual number of wet days (or wet hours) and mean annual wet-day (or wet-hour) intensity at the native 4-km resolution. We set all precipitation intensities bellow 0.1 mm/hr to zero. Light drizzle, which accounts for around 2% of the total precipitation volume in CONUS-404 is therefore excluded from this study. A wet hour is defined as an hour with at least 0.1 mm of accumulated precipitation. A wet day is defined as a day with at least one wet hour. The mean annual wet-day (or wet-hour) intensity is the mean precipitation intensity over all the wet days (or wet hours) of the year. We also compute for each year the fraction of wet hours with intensities above three different threshold values, defined in each pixel as $2 \times \bar{R}_{D1}$, $4 \times \bar{R}_{D1}$ and $8 \times \bar{R}_{D1}$, where \bar{R}_{D1} is the average wet-hour intensity during the first decade of the analysis (D1, 1991–2001) in the corresponding pixel. While the CONUS simulation domain comprises more than one million 4-km pixels, we divided the land areas of the domain into 7,477 surface elements (“surfels”) of dimensions 40 km by 40 km (10 by 10 pixels), and aggregated the annual statistics within each surfel before extracting trends. Such spatial aggregation of pixel statistics reduces the effect of the internal year-to-year variability for more robust trend estimation and improved statistical significance. For all statistics and all surfels, linear trends are extracted by least squares regression of the annual values $X(y)$ against the year y . The regressed line $\hat{X}(y)$ follows the equation:

$$\hat{X}(y) = 0.1 \alpha (y - 1991) + \beta \quad (1)$$

The regressed trends are characterized by the slope coefficient α , expressed in mm dec^{-1} when X represents precipitation volume or intensity, or in dec^{-1} when X represents the number of wet days (or wet hours). In the following, the relative slope coefficient α' in percent per decade is often used instead of the absolute slope coefficient α to characterize the trends:

$$\alpha' = \frac{\alpha}{\bar{X}_{D1}} \quad (2)$$

where \bar{X}_{D1} represents the mean value of the variable of interest over the first decade of the analysis period (1991–2000).

In each surfel and for each variable of interest the p -value of the trend has been estimated with three different methods: t -test, Mann-Kendall test and Monte Carlo permutations. As the three methods produced highly-consistent p -values (see Figures S1 and S2 in Supporting Information S1) only t -test-derived p -values are reported below. Trends with a p -value lower than 0.05 are considered statistically significant.

The trend analysis was also performed at a degraded resolution, by spatially aggregating the CONUS-404 data at a 40 km resolution before performing the analysis. The objective is to demonstrate the effect of data resolution on the magnitude and statistical significance of the trends. The results of this analysis at a degraded resolution are provided in Supporting Information S1 (Figure S3 in Supporting Information S1).

2.3. Statistical Distribution of Precipitation Intensities

The statistical distributions of wet-hour precipitation intensities at 4-km resolution are represented through probability of exceedance (PoE) curves. Changes in the distribution between the first decade of the analysis period (D1, 1991–2000) and the last decade (D3, 2013–2022) are assessed through the ratio of the PoEs $\frac{\text{PoE}_{D3}(R)}{\text{PoE}_{D1}(R)}$ as a function of the intensity R . The ratio of the PoEs at intensity R tells us how many times more frequently (or less frequently) the R value was exceeded during the D3 decade as compared to the D1 decade.

Changes in the distribution between the D1 and D3 decades are also represented through the $\frac{Q_{D3}(F)}{Q_{D1}(F)}$ quantile ratio, where $Q_{D1}(F)$ and $Q_{D3}(F)$ are the intensity values associated with the F -rank quantile of the D1 and D2 distributions respectively.

2.4. Spatial and Temporal Fourier Power Spectral Densities

The space-time dynamics of the 1-hr 4-km precipitation fields are analyzed through their spatial and temporal Fourier power spectral densities (PSDs). The temporal PSDs of the hourly precipitation time series are computed in each 4-km pixel and are then spatially averaged over the region of interest. The spatial PSDs are computed from the 4-km precipitation maps in the region of interest, for each hour of the 1991–2022 period, and are then temporally averaged over specific periods of interest. The two-dimensional spatial power spectra, defined in polar coordinates as functions of the spatial wavenumber and the azimuthal direction, are averaged over all azimuthal directions to produce the omnidirectional spatial PSD as a univariate function of the spatial wavenumber. For easier interpretation, the spatial and temporal PSDs are shown as functions of temporal period and spatial wavelength, respectively, instead of frequency and wavenumber. Changes in the spatial and temporal PSDs between D1 and D3 are represented through the $\frac{\text{PSD}_{D3}}{\text{PSD}_{D1}}$ ratio.

3. Results

3.1. Trends in Precipitation Occurrence and Intensity at Daily and Hourly Scales Over CONUS

Relative trends in the annual precipitation volume, number of wet days, number of wet hours, mean wet-day intensity and mean wet-hour intensity are reported in Figure 1 for each one of the 7,477 surfels of the study domain. For the annual precipitation volume, 63% of the surfels show a positive trend and 37% a negative trend. Negative trends are essentially found in the South-West; positive trends are found in the North (Southern Canada and North-East US). However, when considering solely statistically significant trends (p -value < 0.05), only 0.4% of the surfels show a significant negative trend and 8.2% a significant positive trend (and 91% of the surfels do not show statistically significant trends). Notably, the strong negative trends in the South-West are deemed not statistically significant in most surfels because of the strong year-to-year variability of the precipitation volume in this region, where a few exceptionally dry or exceptionally wet years can drive the trend.

When breaking down the annual precipitation volume into the number of wet days and mean wet-day intensity, it appears that the decreasing trend in precipitation volume in the South-West essentially reflects a decrease in the number of wet days. In contrast, the increasing volume trends in the North are associated with an increase of wet-day intensity, with little variation in the number of wet days. Most of these trends are however not statistically significant, only 6.1% of the surfels show a statistically significant trend in the number of wet days (mostly increasing trends in the Canadian Prairie region and local clusters of decreasing trends in the South-Western US), and 7.5% in the mean wet-day intensity (scattered across the whole study area). These rates of statistically significant trends at the 0.05 level are close to the 5% false-positive rate expected under the null hypothesis.

Now focusing on the hourly statistics, the number of wet hours, similarly to the number of wet days, show decreasing trends in the South-West. These trends are however again deemed essentially non-significant (only 0.8% of the surfels show a significant decreasing trend, which is less than what is expected on average under the null hypothesis). Most interestingly, at the 1-hr resolution, 79% of the surfels of CONUS show an increase in the mean wet-hour intensity, and 17% (of all surfels) show a statistically significant increase (nearly 7 times more than what would be expected under the null hypothesis). The fractional area of CONUS showing a statistically significant increase in the mean wet-hour intensity is 2.5 times larger than the fractional area showing a statistically significant increase in the mean wet-day intensity. The increasing wet-hour intensity trends with the greatest magnitude are found in the Midwest and Northern Prairie.

1991-2022 precipitation trends in CONUS-404

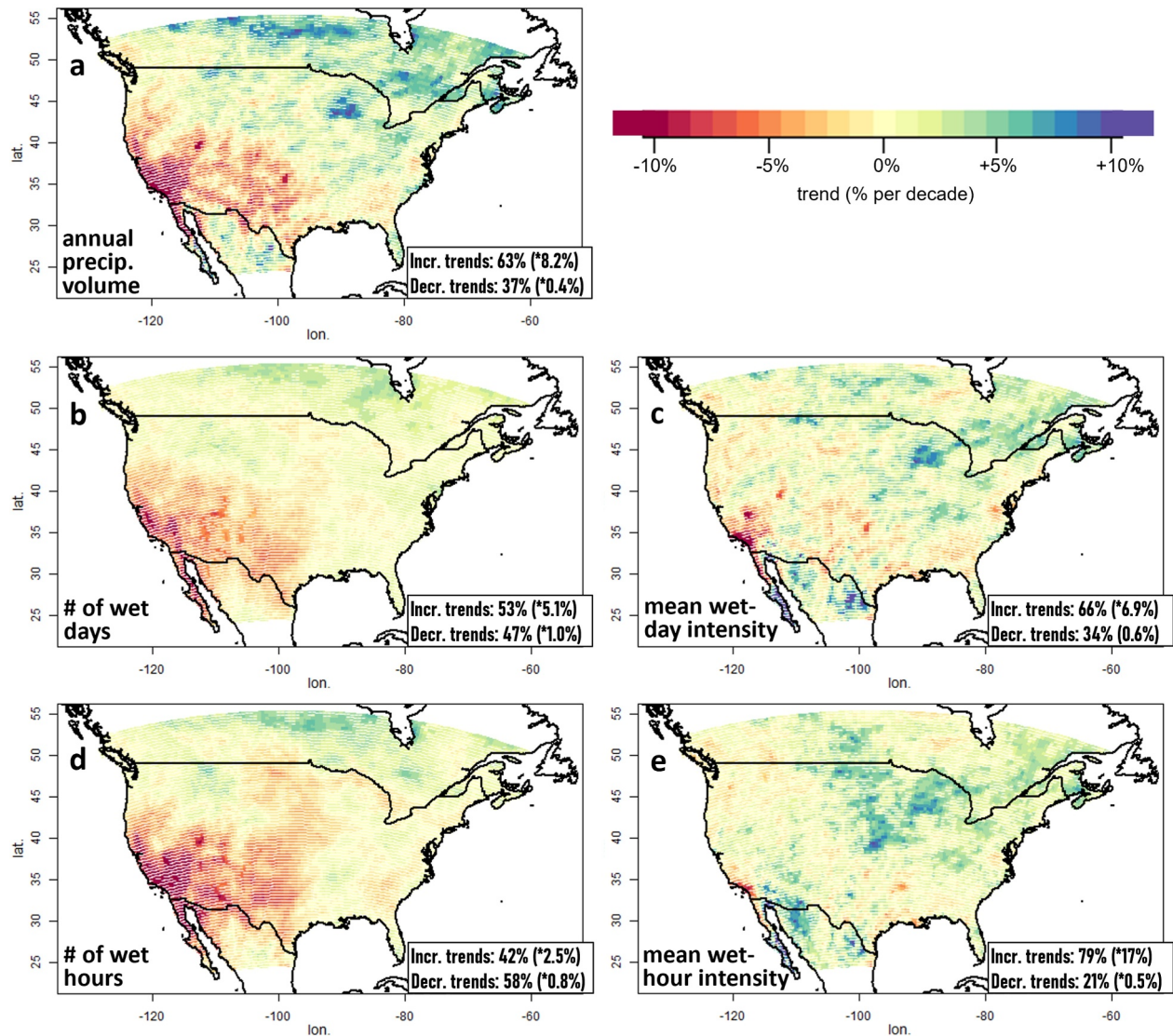


Figure 1. Maps of the relative trends in annual precipitation volume (a), number of wet days (b), mean wet-day intensity (c), number of wet hours (d), and mean wet-hour intensity (e), for the 1991–2022 period. White shading is applied in regions where trends are not significant at the 0.05 level. The fractions of increasing and decreasing trends are indicated for each map, the fractions of statistically significant increasing and decreasing trends are indicated in parentheses. The relative trends are shown in % per decade, with respect to the average value over the first decade of the analysis period (1991–2000).

The above trend analysis was repeated at a degraded 40-km resolution. The results are provided as Figure S3 in Supporting Information S1. The results are consistent in terms of trend patterns, but the relative magnitudes and statistical significances of the trends are generally lower at the 40-km resolution than at the 4-km resolution.

Focusing on the region with the most salient trends, we define the Midwest as the region with -108° to -80° longitudes and 38° – 49° latitudes (rectangle in Figure 2c) for further analyses of precipitation trends. Figure 2d shows the 1991–2022 time series of the annual mean wet-hour intensity at 4-km resolution in the Midwest. The wet-hour intensity increases at an average rate of $0.035 \text{ mm h}^{-1} \text{ dec}^{-1}$, which corresponds to a $3.3\% \text{ dec}^{-1}$ increase with respect to the 1991–2000 average wet-hour intensity. This spatially-averaged trend in the Midwest is statistically significant with a p -value of 3×10^{-4} .

To assess changes in the distribution of wet-hour intensities beyond the mean, we now focus on the fraction of wet hours with intensities above the $2 \times \bar{R}_{D1}$, $4 \times \bar{R}_{D1}$ and $8 \times \bar{R}_{D1}$ thresholds. The panels a, b and c of Figure 2

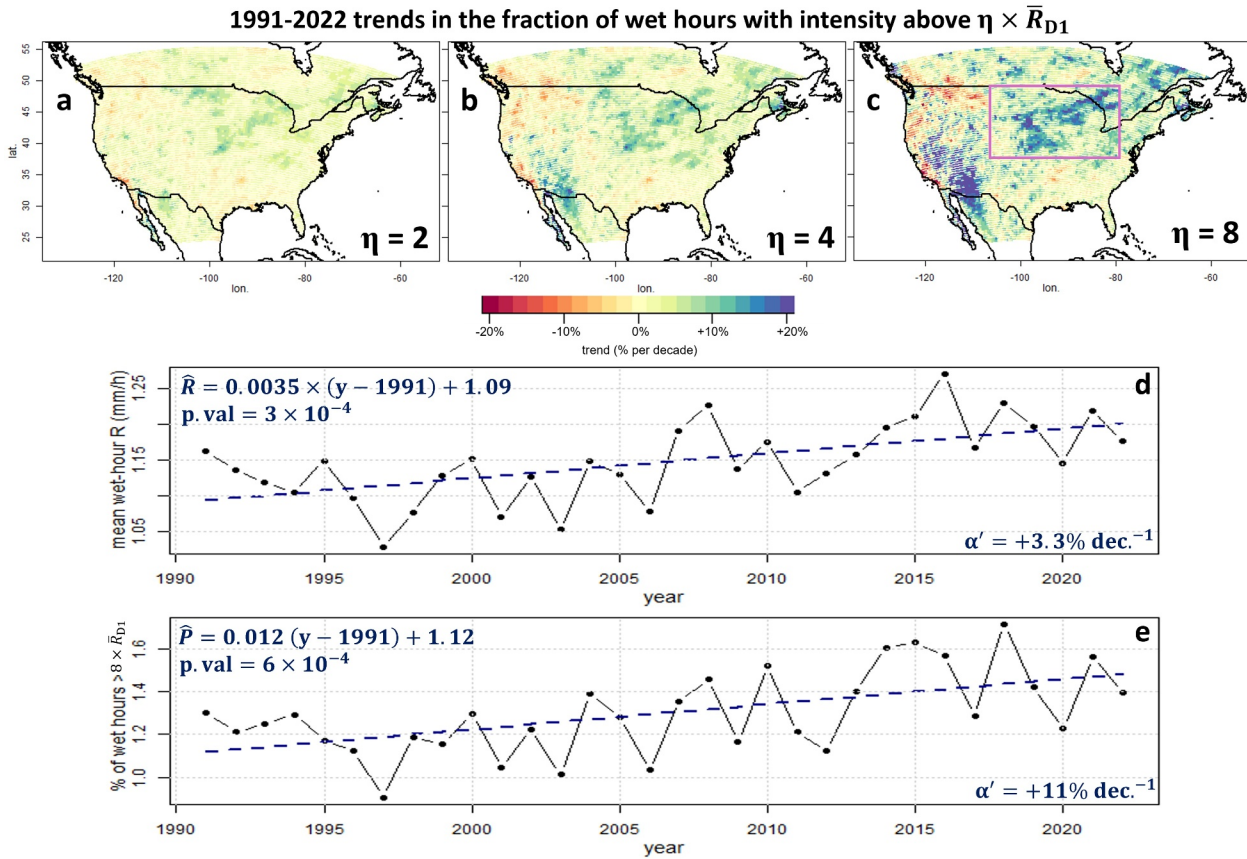


Figure 2. (a, b and c), Maps of the relative trends in the fraction of wet hours with intensity above $2 \times \bar{R}_{D1}$, $4 \times \bar{R}_{D1}$ and $8 \times \bar{R}_{D1}$ respectively, for the 1991–2022 period, where \bar{R}_{D1} is, for each surfel, the mean wet-hour intensity during the first decade of the analysis period. White shading is applied in regions where trends are not significant at the 0.05 level. (d) Time series of the annual mean wet-hour intensity in the Midwest region (delineated by the rectangle in panel c), with regressed linear trend for the 1991–2022 period. (e) Time series of the annual fraction of wet hours with intensity above $8 \times \bar{R}_{D1}$ in the Midwest region, with regressed linear trend for the 1991–2022 period. The relative slope coefficient α' in panels d and e derives from Equation 2.

show the maps of the 1991–2022 relative trends in the fraction of wet hours with intensities above the three intensity thresholds. While the spatial patterns of the trends are similar for the different thresholds, and generally follow the spatial pattern of the mean wet-hour intensity trends, we note that, the higher the threshold, the greater the relative magnitude of the increasing trends, with locally up to a +25% per decade increase of the fraction of wet hours above $8 \times \bar{R}_{D1}$. In the Midwest region, the fraction of wet hours above $8 \times \bar{R}_{D1}$ is found to have increased at an average rate of +11% per decade (with respect to the 1991–2000 mean fraction) over the 1991–2022 period (Figure 2-e).

3.2. Statistical Distribution of 4-km Hourly Precipitation Intensities in the Midwest: 2013–2022 Decade Versus 1991–2000 Decade

In this section, we further analyze changes in the statistical distribution of the 4-km wet-hour intensities in the Midwest, by comparing the statistics for the first decade of the analysis period (D1, 1991–2000) with the statistics for the last decade (D3, 2013–2022). Figure 3a shows a comparison of the respective PoE curves for the two decades, Figure 3b shows the $\frac{PoE_{D3}(R)}{PoE_{D1}(R)}$ ratio as a function of intensity R , and Figure 3-c shows the $\frac{Q_{D3}(F)}{Q_{D1}(F)}$ ratio as a function of the $Q_{D1}(F)$ quantile value (see Section 2.3). One can see that, the greater the intensity, the greater the difference between PoE_{D3} and PoE_{D1} . Between the 0.1 mm/hr and 1 mm/hr intensities, the PoE ratio remains relatively close to 1, revealing that the distribution remained relatively stable for low intensities. At intensity 10 mm/hr, the PoE_{D3} is 1.25 times greater than PoE_{D1} (+25% increase). At intensity 50 mm/hr the increase in the PoE between the two decades is +55%.

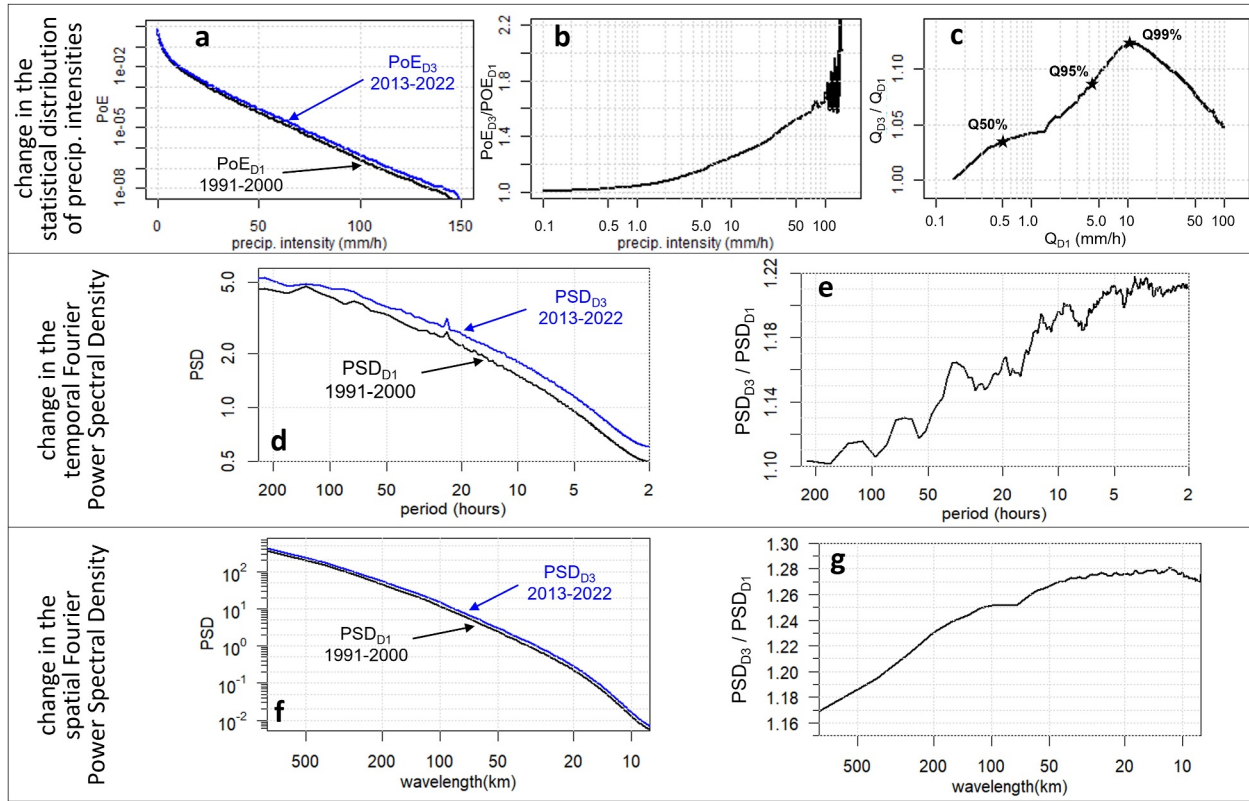


Figure 3. Comparison of precipitation statistics at 1-hr and 4-km resolution in the Midwest between the 1991–2000 decade (D1) and the 2013–2022 decade (D3). (a) Probability of exceedance (PoE) as a function of the wet-hour intensity R , for D1 (black curve) and D3 (blue curve). (b) PoE ratio curve $\frac{\text{PoE}_{D3}(R)}{\text{PoE}_{D1}(R)}$. (c) Quantile to quantile ratio $\frac{Q_{D3}(F)}{Q_{D1}(F)}$ as a function of $Q_{D1}(F)$, where $Q_{D1}(F)$ and $Q_{D3}(F)$ are the values of the (empirically estimated) F -rank quantile of the distribution of wet-hour intensities, for D1 and D3 respectively (see Section 2.3). The Q50%, Q95% and Q99% quantiles are marked on the curve. (d) Temporal Fourier power spectral density functions (PSD) of the hourly precipitation time series, for D1 (black curve) and D3 (blue curve). (e) PSD ratio $\frac{\text{PSD}_{D3}(p)}{\text{PSD}_{D1}(p)}$ as a function of the temporal period p . (f) Omnidirectional spatial Fourier power spectral density functions (PSD) of the hourly precipitation maps, for D1 (black curve) and D3 (blue curve). (g) PSD ratio $\frac{\text{PSD}_{D3}(\lambda)}{\text{PSD}_{D1}(\lambda)}$ as a function of the spatial wavelength λ .

The fact that the Q_{D3}/Q_{D1} ratio is not a constant (Figure 3-c) indicates that the D3 distribution cannot be obtained by linearly scaling the D1 intensity values with a constant coefficient. The Q_{D3}/Q_{D1} ratio curve is found to increase with quantile values up to the Q99% quantile at which it reaches a peak value of 1.13, meaning that the intensity value associated with Q99% is 13% greater for D3 than for D1 (12.2 mm/hr against 10.8 mm/hr). The median value of the distribution (Q50%), on the other hand, only sees a 3.8% amplification between D1 and D3. This nonlinear amplification of precipitation intensities, with intensity values being amplified at a higher rate for higher quantiles is consistent with what has been reported in the literature for CONUS and in other regions of the globe (Feng et al., 2016; Fowler et al., 2021). We note however that, in our case, the monotonic relationship between quantile values and amplification rate only holds up to Q99%, and that quantiles above Q99% are amplified at a decreasing rate with increasing intensity values.

3.3. Spatial and Temporal Spectral Characteristics of Precipitation in the Midwest: 2013–2022 Decade Versus 1991–2000 Decade

In this section, changes in the space-time dynamics of precipitation are quantified through temporal and spatial Fourier spectral analyses of the 1-hr 4-km precipitation intensity fields. The spatial and temporal Fourier PSD functions allow us to non-parametrically detect and quantify changes in space-time dynamics of precipitation (Guiloteau et al., 2025).

Here also, the statistics for the 2013–2022 decade (D3) are compared to those of the 1991–2000 decade (D1), in the Midwest. From panels *d* and *e* of Figure 3, one can see that, at all Fourier periods and wavelengths, the D3 PSD is

higher than the D1 PSD (the $\frac{\text{PSD}_{D3}}{\text{PSD}_{D1}}$ ratio is greater than 1), reflecting an overall increase in the variability (variance) of the 1-hr 4-km precipitation intensities between D1 and D3, across all spatial and temporal scales. Interestingly, the magnitude of the PSD increase between D1 and D3 is greater at shorter periods and shorter wavelengths, revealing that the average amplitude of short-lived small-sized precipitation features has increased at a higher rate than that of large long-lived features. Specifically, as the Fourier period gets shorter, the $\frac{\text{PSD}_{D3}}{\text{PSD}_{D1}}$ ratio gets larger, from a 1.10 value (meaning a +10% increase of the PSD between D1 and D3) at periods longer than 100 hr, down to the 6-hr period at which the PSD ratio reaches a plateau around a value of 1.21 (+21% increase of the PSD between D1 and D3). The $\frac{\text{PSD}_{D3}}{\text{PSD}_{D1}}$ ratio also gets larger with shorter Fourier wavelengths, down to the 50-km wavelength, where it plateaus between 1.27 and 1.28 (+27% to +28% increase of the PSD between D1 and D3).

The spectral analysis demonstrates a scale-dependence in the magnitude of the change in precipitation statistics; the changes are more pronounced at finer spatial and temporal scales. The PSD having increased at a higher rate at shorter periods and shorter wavelengths corresponds to a decrease of the spectral slope (slope of the PSD curves) between D1 and D3. Lower spectral slopes in precipitation fields are generally interpreted as a signature of increasing convective activity and atmospheric instability (Harris et al., 2001; Willeit et al., 2015; Wong & Skamarock, 2016).

4. Summary of Findings

The analysis of precipitation statistics in the CONUS-404 hydroclimate reanalysis at 4-km and 1-hr resolution reveals an increase of mean precipitation intensity during wet hours for the 1991–2022 period, over 79% of the CONUS domain, with 17% of the domain showing a statistically significant increase at the 0.05 level (against 0.2% statistically significant decreasing trends). The intensification trends are particularly pronounced in the Midwest where the average rate of increase is $+0.035 \text{ mm h}^{-1} \text{ dec}^{-1}$ ($+3.3\% \text{ dec}^{-1}$ with respect to the 1991–2000 mean wet-hour intensity). This rate of increase is largely above what is predicted by the Clausius-Clapeyron relationship, as trends in mean annual air temperature reported in the literature are of the order of $0.1\text{--}0.25 \text{ K dec}^{-1}$ for the recent decades in the Midwest (U.S. Global Change Research Program, 2023). While the relative magnitudes of the trends in the annual number of wet hours are quite similar to that of the trends in the wet-hour intensities, the former show much lower levels of statistical significance. These low significance levels come from the very high year-to-year internal variability of the number of wet hours and the limited length of the analysis period (32 years).

The comparisons of the distribution of hourly precipitation intensities and of the temporal and spatial Fourier PSDs between the first decade (1991–2000) and the last decade (2013–2022) revealed that the intensification of precipitation rates in the Midwest is nonlinear, intensity-dependent and scale-dependent. While the median value of the distribution of hourly precipitation intensities at 4-km resolution has increased by 3.8% between the first and the last decade, the value associated with the 99th percentile has increased by 13%. The Fourier PSDs show that, between the first and last decade, short-lived small-sized precipitation features have seen a more pronounced amplification than larger longer-lived features, with a maximal increase of spectral power at wavelengths shorter than 50 km and periods shorter than 6 hr. This last result is consistent with the finding that the magnitude and statistical significance of the intensity trends drop substantially when performing the statistical analysis at degraded resolutions (40 km/24 hr).

5. Discussion

The nonlinear scaling of precipitation intensities between the first decade (1991–2000) and the last decade (2013–2022) of the analysis period in the Midwest, and the changes in the space-time structure of precipitation fields revealed by the temporal and spatial Fourier PSDs, indicate a change in precipitation dynamics, consistent with the hypothesis of a shift toward a higher convective fraction and higher convective intensity of precipitating clouds. Given the typical size and lifetime of convective cells, it is not surprising that the signature of this shift is more perceptible at high resolution (e.g., 1 hr and 4 km) than at coarser resolutions (e.g., 24 hr and 40 km).

At coarse scales, changes related to increased convection may in fact be only perceptible when focusing on organized mesoscale convective systems (MCSs) or mesoscale convective complexes that can produce

widespread high-intensity precipitation over periods exceeding 12 hr (Feng et al., 2016; Hu et al., 2020; Schumacher & Rasmussen, 2020). This is likely one reason why studies reporting historical trends in precipitation at coarse resolutions have often focused on extremes (e.g., Alexander et al., 2020; Harrison et al., 2019; Papalexiou & Montanari, 2019; Sun et al., 2021; Thackeray et al., 2022; Wang et al., 2023), which, most of the time, are associated to MCSs (Roca et al., 2014; Roca & Fiolleau, 2020; Zhao, 2022).

It is worth noting that the nature of the changes reported in the present analysis of historical data over CONUS, that is, an increase of the mean wet-hour intensity and an amplification of the fine-scale variability of precipitation, over the Midwest in particular, is consistent with the changes reported in Guilloteau et al. (2025) between historical (1981–2020) and future (2041–2080) hydroclimate simulations at 6-km and 1-hr resolution over the western half of CONUS under the RCP8.5 scenario, and with other published studies focusing on future hydroclimate simulations (e.g., Dallan et al., 2024; Westra et al., 2014). The present study tends to indicate that the hypothesized shift toward higher convective fraction and higher convective intensity in precipitating clouds under global warming (Haerter & Berg, 2009), which has been confirmed by model simulations (Moseley et al., 2016; Singleton & Toumi, 2013), is already detectable in high-resolution historical data sets in certain regions of the world. Such trends may however be less detectable at the coarse resolutions of global products (observational products and reanalysis) and global climate models.

Conflict of Interest

The authors declare no conflicts of interest relevant to this study.

Data Availability Statement

The CONUS-404 data set (Rasmussen, Liu, et al., 2023) used in the present study is publicly available on the NSF NCAR Research Data Archive.

Acknowledgments

This work was supported by NASA (Grants 80NSSC22K0597 and 80NSSC23K1304), the National Science Foundation (Grant IIS2324008), and by the Office of Science of the U.S. Department of Energy Biological and Environmental Research through the HyperFACETS project within the Regional and Global Model Analysis and Multisector Dynamics program areas. The Pacific Northwest National Laboratory is operated for the Department of Energy by the Battelle Memorial Institute under contract DE-AC05-76RL01830. The authors thank the two reviewers for their constructive comments and suggestions.

References

- Adhikari, P., Geerts, B., Rahimi-Esfarjani, S., Smith, K., Shuman, B. N., & Schneider, T. L. (2024). Evaluation of the mountain hydroclimate across the western United States in dynamically downscaled climate models. *Journal of Hydrometeorology*, 25(12), 1877–1894. <https://doi.org/10.1175/JHM-D-24-0063.1>
- Alexander, L. V., Bador, M., Roca, R., Contractor, S., Donat, M. G., & Nguyen, P. L. (2020). Intercomparison of annual precipitation indices and extremes over global land areas from in situ, space-based and reanalysis products. *Environmental Research Letters*, 15(5), 055002. <https://doi.org/10.1088/1748-9326/ab79e2>
- Ayat, H., Evans, J. P., & Behrangi, A. (2021). How do different sensors impact IMERG precipitation estimates during hurricane days? *Remote Sensing of Environment*, 259, 112417. <https://doi.org/10.1016/j.rse.2021.112417>
- Berg, P., Moseley, C., & Haerter, J. O. (2013). Strong increase in convective precipitation in response to higher temperatures. *Nature Geoscience*, 6(3), 181–185. <https://doi.org/10.1038/ngeo1731>
- Bromwich, D. H., Ensign, A., Wang, S. H., & Zou, X. (2024). Major artifacts in ERA5 2-m air temperature trends over Antarctica prior to and during the modern satellite era. *Geophysical Research Letters*, 51(21), e2024GL111907. <https://doi.org/10.1029/2024GL111907>
- Buschow, S. (2024). Tropical convection in ERA5 has partly shifted from parameterized to resolved. *Quarterly Journal of the Royal Meteorological Society*, 150(758), 436–446. <https://doi.org/10.1002/qj.4604>
- Carvalho, L. M. (2020). Assessing precipitation trends in the Americas with historical data: A review. *Wiley Interdisciplinary Reviews: Climate Change*, 11(2), e627. <https://doi.org/10.1002/wcc.627>
- Dallan, E., Marra, F., Fossier, G., Marani, M., & Borga, M. (2024). Dynamical factors heavily modulate the future increase of sub-daily extreme precipitation in the alpine-mediterranean region. *Earth's Future*, 12(12), e2024EF005185. <https://doi.org/10.1029/2024ef005185>
- Da Silva, N. A., & Haerter, J. O. (2025). Super-Clausius–Clapeyron scaling of extreme precipitation explained by shift from stratiform to convective rain type. *Nature Geoscience*, 18(5), 382–388. <https://doi.org/10.1038/s41561-025-01686-4>
- Doviak, R. J., Bringi, V., Ryzhkov, A., Zahrai, A., & Zrnić, D. (2000). Considerations for polarimetric upgrades to operational WSR-88D radars. *Journal of Atmospheric and Oceanic Technology*, 17(3), 257–278. [https://doi.org/10.1175/1520-0426\(2000\)017<0257:CFPUTO>2.0.CO;2](https://doi.org/10.1175/1520-0426(2000)017<0257:CFPUTO>2.0.CO;2)
- Eldardiry, H., Habib, E., Zhang, Y., & Grascel, J. (2017). Artifacts in stage IV NWS real-time multisensor precipitation estimates and impacts on identification of maximum series. *Journal of Hydrologic Engineering*, 22(5), E4015003. [https://doi.org/10.1061/\(asce\)jhe.1943-5584.0001291](https://doi.org/10.1061/(asce)jhe.1943-5584.0001291)
- Emmanouil, S., Langousis, A., Nikolopoulos, E. I., & Anagnostou, E. N. (2022). The spatiotemporal evolution of rainfall extremes in a changing climate: A CONUS-wide assessment based on multifractal scaling arguments. *Earth's Future*, 10(3), e2021EF002539. <https://doi.org/10.1029/2021EF002539>
- Feng, Z., Leung, L. R., Hagos, S., Houze, R. A., Burleyson, C. D., & Balaguru, K. (2016). More frequent intense and long-lived storms dominate the springtime trend in central US rainfall. *Nature Communications*, 7(1), 13429. <https://doi.org/10.1038/ncomms13429>
- Fowler, H. J., Lenderink, G., Prein, A. F., Westra, S., Allan, R. P., Ban, N., et al. (2021). Anthropogenic intensification of short-duration rainfall extremes. *Nature Reviews Earth & Environment*, 2(2), 107–122. <https://doi.org/10.1038/s43017-020-00128-6>
- Gu, G., & Adler, R. F. (2023). Observed variability and trends in global precipitation during 1979–2020. *Climate Dynamics*, 61(1), 131–150. <https://doi.org/10.1007/s00382-022-06567-9>
- Guilloteau, C., Chen, X., Leung, L. R., & Foufoula-Georgiou, E. (2025). Amplified mesoscale and submesoscale variability and increased concentration of precipitation under global warming over western North America. *Journal of Climate*, 38(11), 2525–2542. <https://doi.org/10.1175/JCLI-D-24-0343.1>

- Guilloteau, C., & Foufoula-Georgiou, E. (2020). Multiscale evaluation of satellite precipitation products: Effective resolution of IMERG. *Satellite precipitation measurement* (Vol. 2, pp. 533–558). https://doi.org/10.1007/978-3-030-35798-6_5
- Guilloteau, C., & Foufoula-Georgiou, E. (2023). Preserving extremes in satellite quantitative precipitation estimates: A matter of scale. In *Proceedings of the IGARSS 2023 IEEE international geoscience and remote sensing symposium* (pp. 662–665). <https://doi.org/10.1109/IGARSS52108.2023.10281499>
- Guilloteau, C., Foufoula-Georgiou, E., & Kummerow, C. D. (2017). Global multiscale evaluation of satellite passive microwave retrieval of precipitation during the TRMM and GPM eras: Effective resolution and regional diagnostics for future algorithm development. *Journal of Hydrometeorology*, 18(11), 3051–3070. <https://doi.org/10.1175/JHM-D-17-0087.1>
- Haerter, J. O., & Berg, P. (2009). Unexpected rise in extreme precipitation caused by a shift in rain type? *Nature Geoscience*, 2(6), 372–373. <https://doi.org/10.1038/ngeo523>
- Harris, D., Foufoula-Georgiou, E., Droegemeier, K. K., & Levit, J. J. (2001). Multiscale statistical properties of a high-resolution precipitation forecast. *Journal of Hydrometeorology*, 2(4), 406–418. [https://doi.org/10.1175/1525-7541\(2001\)002<0406:MSPOAH>2.0.CO;2](https://doi.org/10.1175/1525-7541(2001)002<0406:MSPOAH>2.0.CO;2)
- Harrison, L., Funk, C., & Peterson, P. (2019). Identifying changing precipitation extremes in Sub-Saharan Africa with gauge and satellite products. *Environmental Research Letters*, 14(8), 085007. <https://doi.org/10.1088/1748-9326/ab2cae>
- Hersbach, H., Bell, B., Berrisford, P., Hirahara, S., Horányi, A., Muñoz-Sabater, J., et al. (2020). The ERA5 global reanalysis. *Quarterly Journal of the Royal Meteorological Society*, 146(730), 1999–2049. <https://doi.org/10.1002/qj.3803>
- Hu, H., Leung, L. R., & Feng, Z. (2020). Observed warm-season characteristics of MCS and non-MCS rainfall and their recent changes in the central United States. *Geophysical Research Letters*, 47(6), e2019GL086783. <https://doi.org/10.1029/2019GL086783>
- John, A., Douville, H., Ribes, A., & Yiou, P. (2022). Quantifying CMIP6 model uncertainties in extreme precipitation projections. *Weather and Climate Extremes*, 36, 100435. <https://doi.org/10.1016/j.wace.2022.100435>
- Kidd, C., Becker, A., Huffman, G. J., Muller, C. L., Joe, P., Skofronick-Jackson, G., & Kirschbaum, D. B. (2017). So, how much of the Earth's surface is covered by rain gauges? *Bulletin of the American Meteorological Society*, 98(1), 69–78. <https://doi.org/10.1175/BAMS-D-14-00283.1>
- Li, J., Huo, R., Chen, H., Zhao, Y., & Zhao, T. (2021). Comparative assessment and future prediction using CMIP6 and CMIP5 for annual precipitation and extreme precipitation simulation. *Frontiers in Earth Science*, 9, 687976. <https://doi.org/10.3389/feart.2021.687976>
- Mascaro, G., Farris, S., & Deidda, R. (2025). Evidence of emerging increasing trends in observed subdaily heavy precipitation frequency in the United States. *Geophysical Research Letters*, 52(12), e2024GL114292. <https://doi.org/10.1029/2024gl114292>
- Masunaga, H., Schröder, M., Furuzawa, F. A., Kummerow, C., Rustemeier, E., & Schneider, U. (2019). Inter-product biases in global precipitation extremes. *Environmental Research Letters*, 14(12), 125016. <https://doi.org/10.1088/1748-9326/ab5da9>
- Moseley, C., Hohenegger, C., Berg, P., & Haerter, J. O. (2016). Intensification of convective extremes driven by cloud–cloud interaction. *Nature Geoscience*, 9(10), 748–752. <https://doi.org/10.1038/ngeo2789>
- Nerantzaki, S. D., Abdelmoaty, H. M., Papalexioy, S. M., & Newman, A. J. (2025). The influence of atmospheric drivers, environmental factors, and urban land use on extreme hourly precipitation trends over the CONtiguous United States for 40 years at 4-km resolution (CONUS404). *Science of the Total Environment*, 969, 178407. <https://doi.org/10.1016/j.scitotenv.2025.178407>
- Nguyen, P., Thorstensen, A., Sorooshian, S., Hsu, K., Aghakouchak, A., Ashouri, H., et al. (2018). Global precipitation trends across spatial scales using satellite observations. *Bulletin of the American Meteorological Society*, 99(4), 689–697. <https://doi.org/10.1175/bams-d-17-0065.1>
- North, G. R., & Erukhimova, T. L. (2009). Chap. 9: Air and water. In *Atmospheric thermodynamics: Elementary physics and chemistry* (pp. 99–133). Cambridge University Press.
- O’Gorman, P. A. (2015). Precipitation extremes under climate change. *Current Climate Change Reports*, 1(2), 49–59. <https://doi.org/10.1007/s40641-015-0009-3>
- Panthou, G., Mailhot, A., Laurence, E., & Talbot, G. (2014). Relationship between surface temperature and extreme rainfalls: A multi-time-scale and event-based analysis. *Journal of Hydrometeorology*, 15(5), 1999–2011. <https://doi.org/10.1175/JHM-D-14-0020.1>
- Papalexioy, S. M., & Montanari, A. (2019). Global and regional increase of precipitation extremes under global warming. *Water Resources Research*, 55(6), 4901–4914. <https://doi.org/10.1029/2018WR024067>
- Petković, V., Brown, P. J., Berg, W., Randel, D. L., Jones, S. R., & Kummerow, C. D. (2023). Can we estimate the uncertainty level of satellite long-term precipitation records? *Journal of Applied Meteorology and Climatology*, 62(8), 1069–1082. <https://doi.org/10.1175/jamc-d-22-0179.1>
- Polasky, A., Sapkota, V., Forest, C. E., & Fuentes, J. D. (2025). Discrepancies in precipitation trends between observational and reanalysis datasets in the Amazon Basin. *Scientific Reports*, 15(1), 7268. <https://doi.org/10.1038/s41598-025-87418-5>
- Rajagopal, M., Zipser, E., Huffman, G., Russell, J., & Tan, J. (2021). Comparisons of IMERG version 06 precipitation at and between passive microwave overpasses in the tropics. *Journal of Hydrometeorology*, 22(8), 2117–2130. <https://doi.org/10.1175/JHM-D-20-0226.1>
- Rasmussen, R. M., Chen, F., Liu, C. H., Ikeda, K., Prein, A., Kim, J., et al. (2023). CONUS404: The NCAR–USGS 4-km long-term regional hydroclimate reanalysis over the CONUS. *Bulletin of the American Meteorological Society*, 104(8), E1382–E1408. <https://doi.org/10.1175/BAMS-D-21-0326.1>
- Rasmussen, R. M., Liu, C., Ikeda, K., Chen, F., Kim, J.-H., Schneider, T., et al. (2023). Four-kilometer long-term regional hydroclimate reanalysis over the conterminous United States (CONUS) [Dataset]. *Research Data Archive at the National Center for Atmospheric Research, Computational and Information Systems Laboratory*. <https://doi.org/10.5065/ZYY0-Y036>
- Roca, R., Aublanc, J., Chambon, P., Fiolleau, T., & Viltard, N. (2014). Robust observational quantification of the contribution of mesoscale convective systems to rainfall in the tropics. *Journal of Climate*, 27(13), 4952–4958. <https://doi.org/10.1175/JCLI-D-13-00628.1>
- Roca, R., & Fiolleau, T. (2020). Extreme precipitation in the tropics is closely associated with long-lived convective systems. *Communications Earth & Environment*, 1(1), 18. <https://doi.org/10.1038/s43247-020-00015-4>
- Schumacher, R. S., & Rasmussen, K. L. (2020). The formation, character and changing nature of mesoscale convective systems. *Nature Reviews Earth & Environment*, 1(6), 300–314. <https://doi.org/10.1038/s43017-020-0057-7>
- Singleton, A., & Toumi, R. (2013). Super-Clausius–Clapeyron scaling of rainfall in a model squall line. *Quarterly Journal of the Royal Meteorological Society*, 139(671), 334–339. <https://doi.org/10.1002/qj.1919>
- Sun, Q., Zhang, X., Zwiers, F., Westra, S., & Alexander, L. V. (2021). A global, continental, and regional analysis of changes in extreme precipitation. *Journal of Climate*, 34(1), 243–258. <https://doi.org/10.1175/JCLI-D-19-0892.1>
- Thackeray, C. W., Hall, A., Norris, J., & Chen, D. (2022). Constraining the increased frequency of global precipitation extremes under warming. *Nature Climate Change*, 12(5), 441–448. <https://doi.org/10.1038/s41558-022-01329-1>
- U.S. Global Change Research Program. (2023). Fifth national climate assessment. <https://doi.org/10.7930/NCA5.2023>

- Wang, T., Li, Z., Ma, Z., Gao, Z., & Tang, G. (2023). Diverging identifications of extreme precipitation events from satellite observations and reanalysis products: A global perspective based on an object-tracking method. *Remote Sensing of Environment*, 288, 113490. <https://doi.org/10.1016/j.rse.2023.113490>
- Westra, S., Fowler, H. J., Evans, J. P., Alexander, L. V., Berg, P., Johnson, F., et al. (2014). Future changes to the intensity and frequency of short-duration extreme rainfall. *Reviews of Geophysics*, 52(3), 522–555. <https://doi.org/10.1002/2014RG000464>
- Willeit, M., Amorati, R., Montani, A., Pavan, V., & Tesini, M. S. (2015). Comparison of spectral characteristics of precipitation from radar estimates and COSMO-model predicted fields. *Meteorology and Atmospheric Physics*, 127(2), 191–203. <https://doi.org/10.1007/s00703-014-0359-8>
- Williams, A. P., McKinnon, K. A., Anchukaitis, K. J., Gershunov, A., Varuolo-Clarke, A. M., Clemesha, R. E., & Liu, H. (2024). Anthropogenic intensification of cool-season precipitation is not yet detectable across the Western United States. *Journal of Geophysical Research: Atmospheres*, 129(12), e2023JD040537. <https://doi.org/10.1029/2023JD040537>
- Wong, M., & Skamarock, W. C. (2016). Spectral characteristics of convective-scale precipitation observations and forecasts. *Monthly Weather Review*, 144(11), 4183–4196. <https://doi.org/10.1175/MWR-D-16-0183.1>
- Yang, D., Goodison, B. E., Metcalfe, J. R., Golubev, V. S., Bates, R., Pangburn, T., & Hanson, C. L. (1998). Accuracy of NWS 8 standard nonrecording precipitation gauge: Results and application of WMO intercomparison. *Journal of Atmospheric and Oceanic Technology*, 15(1), 54–68. [https://doi.org/10.1175/1520-0426\(1998\)015<0054:AONSNP>2.0.CO;2](https://doi.org/10.1175/1520-0426(1998)015<0054:AONSNP>2.0.CO;2)
- Zaitchik, B. F., Rodell, M., Biasutti, M., & Seneviratne, S. I. (2023). Wetting and drying trends under climate change. *Nature Water*, 1(6), 502–513. <https://doi.org/10.1038/s44221-023-00073-w>
- Zhang, Y., & Wang, K. (2023). Global precipitation system scale increased from 2001 to 2020. *Journal of Hydrology*, 616, 128768. <https://doi.org/10.1016/j.jhydrol.2022.128768>
- Zhao, M. (2022). A study of AR-TS-and MCS-associated precipitation and extreme precipitation in present and warmer climates. *Journal of Climate*, 35(2), 479–497. <https://doi.org/10.1175/JCLI-D-21-0145.1>